



# Direct evidence that Ataxin-2 is a translational activator mediating cytoplasmic polyadenylation

Received for publication, April 12, 2020, and in revised form, September 13, 2020. Published, Papers in Press, September 28, 2020, DOI 10.1074/jbc.RA120.013835

Hiroto Inagaki<sup>1</sup>, Nao Hosoda<sup>1</sup>, Hitomi Tsuji<sup>2</sup>, and Shin-ichi Hoshino<sup>1,\*</sup>

From the Departments of <sup>1</sup>Biological Chemistry and <sup>2</sup>Biomedical Science, Graduate School of Pharmaceutical Sciences, Nagoya City University, Nagoya, Japan

Edited by Karin Musier-Forsyth

The RNA-binding protein Ataxin-2 binds to and stabilizes a number of mRNA sequences, including that of the transactive response DNA-binding protein of 43 kDa (TDP-43). Ataxin-2 is additionally involved in several processes requiring translation, such as germline formation, long-term habituation, and circadian rhythm formation. However, it has yet to be unambiguously demonstrated that Ataxin-2 is actually involved in activating the translation of its target mRNAs. Here we provide direct evidence from a polysome profile analysis showing that Ataxin-2 enhances translation of target mRNAs. Our recently established method for transcriptional pulse-chase analysis under conditions of suppressing deadenylation revealed that Ataxin-2 promotes post-transcriptional polyadenylation of the target mRNAs. Furthermore, Ataxin-2 binds to a poly(A)-binding protein PABPC1 and a noncanonical poly(A) polymerase PAPD4 via its intrinsically disordered region (amino acids 906–1095) to recruit PAPD4 to the targets. Post-transcriptional polyadenylation by Ataxin-2 explains not only how it activates translation but also how it stabilizes target mRNAs, including TDP-43 mRNA. Ataxin-2 is known to be a potent modifier of TDP-43 proteinopathies and to play a causative role in the neurodegenerative disease spinocerebellar ataxia type 2, so these findings suggest that Ataxin-2-induced cytoplasmic polyadenylation and activation of translation might impact neurodegeneration (*i.e.* TDP-43 proteinopathies), and this process could be a therapeutic target for Ataxin-2-related neurodegenerative disorders.

The 3'-ends of most eukaryotic mRNAs are modified cotranscriptionally by the addition of a poly(A) tail (1). The poly(A) tail plays crucial roles in gene expression, particularly in translation and mRNA stability (2, 3). These roles are largely mediated by the poly(A)-binding protein cytoplasmic 1 (PABPC1), which specifically covers the poly(A) tail (4). Poly(A)-bound PABPC1 interacts with the cap-binding eukaryotic translation initiation factor 4E (eIF4E) through a scaffold protein, eIF4G, thereby enabling mRNA to form a circular structure (5, 6). By the binding of eukaryotic release factor (eRF)1–eRF3 to the PABPC1–eIF4E–eIF4G complex through interaction with PABPC1 (7), the terminating ribosome could be brought into close proximity with the initiation site. The closed-loop structure is assumed to increase the efficiency of ribosome recruitment for the next round of translation (8). In

fact, it has been demonstrated that translation of the capped mRNA is synergistically activated by the presence of poly(A) tail *in vitro* and *in vivo* (9). PABPC1 also interacts with two deadenylase complexes, Pan2–Pan3 and Caf1–Ccr4–Tob, as well as with eRF1–eRF3 to execute shortening of the poly(A) tail, termed deadenylation (10–14). These interactions are mediated by the C-terminal PABC domain of PABPC1 and PABPC1-interacting motif 2 (PAM2) of eRF3, Pan3, and Tob (10, 12, 15, 16). Deadenylation is mediated by concerted actions of these PAM2-containing proteins; after translation is terminated, eRF1–eRF3 dissociates from PABPC1 bound to the poly(A) tail, and in turn, Pan2–Pan3 and Caf1–Ccr4–Tob associate with PABPC1, leading to the activation of the deadenylases and shortening of the poly(A) tail (as proposed in Refs. 10 and 17). Because deadenylation is the rate-limiting step in the degradation of most mRNAs, regulating the length of the poly(A) tail plays a key role in the control of mRNA stability (17). Accumulating evidence has shown that the stability of each transcript is regulated by sequence-specific RNA-binding proteins that bind to the cis-element, in most cases in the 3'-UTR of mRNA. The tandem CCCH zinc-finger RNA-binding protein TTP (tristetraprolin), which directly binds to adenine/uridine-rich elements (AREs), recruits the Ccr4–Not deadenylase complex to accelerate deadenylation and decay of target mRNAs (18, 19). In a similar manner, cytoplasmic polyadenylation element (CPE)-binding proteins (CPEB and CPEB3) (20, 21), Smaug (22), Pumilio and FBF (PUF) (23), Roquin (24), heterogeneous nuclear ribonucleoprotein A1 (hnRNP A1) (25), CAG triplet repeat RNA-binding protein 1 (CUGBP1) (26), RNA-binding protein mRNA-processing factor (RBPMS) (27), transactive response DNA-binding protein of 43 kDa (TDP-43) (28), and RNA-induced silencing complex (RISC) (29–31) also accelerate deadenylation of the target mRNAs. Thus, RNA-binding protein-mediated accelerated deadenylation of the target mRNA is well-established as a means for negative regulation of gene expression.

However, emerging evidence has suggested that translation is positively regulated by the post-transcriptional polyadenylation of mRNAs. In early development, CPEB promotes translation via cytoplasmic polyadenylation of maternal mRNA that is mediated by poly(A) polymerase-associated domain (PAPD) 4 (32). However, only a limited number of transcripts have been identified to be regulated by the cytoplasmic polyadenylation in somatic cells (33–35).

Spinocerebellar ataxia type 2 (SCA2) gene product, Ataxin-2, is a member of the Like-Sm (LSm) family of RNA-binding

This article contains supporting information.

\*For correspondence: Shin-ichi Hoshino, hoshino@phar.nagoya-cu.ac.jp.

This is an Open Access article under the CC BY license.

15810 *J. Biol. Chem.* (2020) 295(47) 15810–15825

© 2020 Inagaki et al. Published under exclusive license by The American Society for Biochemistry and Molecular Biology, Inc.



proteins and contains a polyglutamine (polyQ) repeat of ~22–23 amino acids in healthy individuals, whereas significant expansion of the polyQ repeat to over 34 amino acids is the genetic cause of SCA2 (36–39). Ataxin-2 intermediate-length polyQ repeat expansions (27–33 amino acids) are associated with increased risk of ALS, a neurodegeneration with abnormal cytoplasmic aggregation of TDP-43 called TDP-43 proteinopathy (40). Ataxin-2 contains PAM2 in its C-terminal region along with the N-terminal LSm domain (41–43), which directly binds to a 3'-UTR of specific mRNAs and promotes its stability and protein production (44). However, it remains unresolved whether Ataxin-2 affects translation of the target mRNAs and how Ataxin-2 stabilizes mRNAs.

Here, we demonstrate that Ataxin-2 enhances translation through post-transcriptional polyadenylation of the targets, including cyclin D1 and TDP-43 mRNAs. Ataxin-2 physically interacts with PABPC1 and PAPD4 and induces lengthening of the poly(A) tail, which leads to the enhancement of translation. These results demonstrate that Ataxin-2–induced post-transcriptional polyadenylation positively regulates target gene expression at both translation and mRNA stability.

## Results

### Ataxin-2 activates translation of the target mRNA through binding to the 3'-UTR

Previous studies demonstrated that Ataxin-2 is involved in translation-required processes, including germline formation, long-term habituation, and circadian rhythm formation. Although there are multiple lines of correlational evidence, it has yet to be determined whether Ataxin-2 directly activates translation of its target mRNAs. To address this issue, we first utilized a tethering strategy in which Ataxin-2 was fused to the coat protein of bacteriophage MS2, and the MS2-binding site was incorporated into a reporter mRNA (Fig. 1A). HEK293T cells were co-transfected with three plasmids; the first harbored the firefly luciferase–MS2bs reporter that contains eight contiguous copies of the MS2-binding site ( $8 \times$  MS2bs) in its 3'-UTR, the second is a reference plasmid expressing *Renilla* luciferase as a transfection/loading control, and the third expresses either MS2-fused 5×Myc-glutathione *S*-transferase (GST) or MS2-fused 5×Myc-Ataxin-2. Tethering of Ataxin-2 to the mRNA resulted in 4.1-fold increase in the level of the reporter protein as compared with that in the control case with GST (Fig. 1B). Under this condition, Ataxin-2 tethering resulted in a 2.0-fold increase in the level of the reporter mRNA as compared with that in the GST control (Fig. 1C). These results are consistent with a previous report showing that Ataxin-2 promotes mRNA stability and protein expression by using the λN-boxB tethering assay system (44). Therefore, it is estimated that Ataxin-2 tethering resulted in a 2.1-fold increase in the translation efficiency of the reporter mRNA, as calculated by normalizing the reporter protein to the mRNA level (Fig. 1D). Protein expression was confirmed by Western blotting (Fig. 1E). To obtain direct evidence showing that Ataxin-2 enhances translation efficiency of the target mRNA, we examined the translation status of the target mRNA by performing polysome profile analysis. HEK293T cells were co-transfected with a reporter

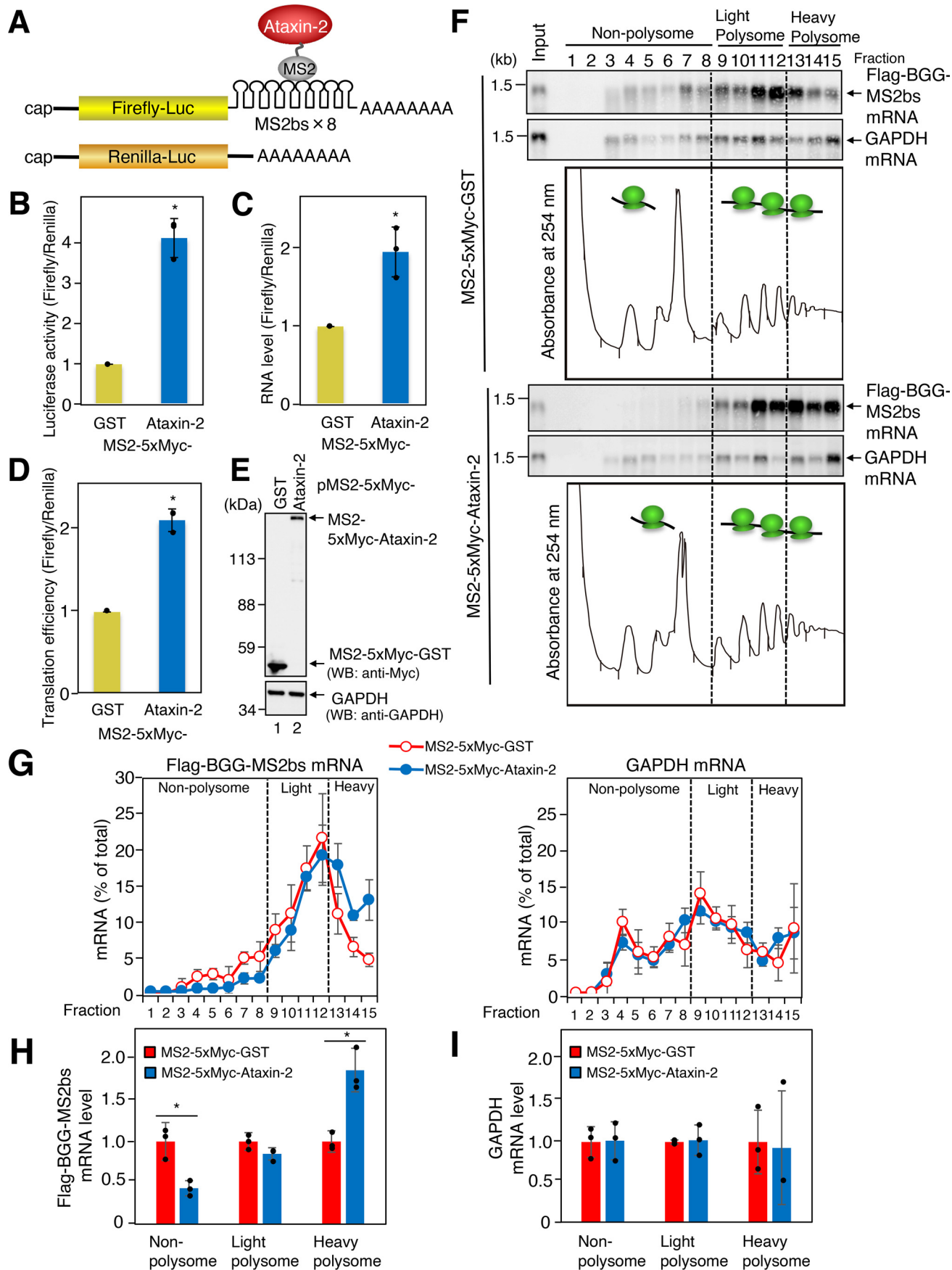
plasmid expressing FLAG-β-globin (BGG)–MS2bs mRNA and a plasmid expressing either MS2-fused 5×Myc-tagged GST or Ataxin-2. The cell lysates were loaded on a 10–50% linear sucrose density gradient and fractionated after ultracentrifugation to separate the polysomes. In terms of overall polysome profiles, no major changes were observed between Ataxin-2 tethering and GST control (Fig. 1F). RNAs extracted from each fraction were subjected to Northern blotting (Fig. 1F), and the levels of FLAG-BGG–MS2bs mRNA in each fraction were measured (Fig. 1G). Ataxin-2 tethering induced a shift in the distribution of the mRNA from nonpolysome fractions to heavy polysome fractions (over six ribosomes on mRNA) along the sucrose gradient (Fig. 1G, left). No such changes were observed for the control GAPDH mRNA (Fig. 1G, right). Calculation of mRNA levels in nonpolysomal, light polysomal, and heavy polysomal fractions showed that tethering of Ataxin-2 resulted in a 2.3-fold reduction in the level of FLAG-BGG–MS2bs mRNA in the nonpolysomal fractions as compared with the GST control, whereas a 1.9-fold increase in the level of FLAG-BGG–MS2bs mRNA in the heavy polysomal fractions (Fig. 1H). The changes were not observed for the control GAPDH mRNA (Fig. 1I). These results strongly suggest that Ataxin-2 promotes mRNA translation by enhancing translation efficiency of the target mRNA.

### Ataxin-2 promotes lengthening of the poly(A) tail of the target mRNA through interaction with PABPC1

Because Ataxin-2 contains PAM2 and binds to PABPC1 (45), it has been suggested that Ataxin-2 may be involved in the regulation of poly(A) tail. The fact that Ataxin-2 increases both translation efficiency and mRNA stability prompted us to consider the idea that poly(A) tail regulation may be involved in the mechanism underlying these Ataxin-2 actions. Consistent with this idea, we noticed that Ataxin-2 increased the size of the target mRNA. When MS2-fused Ataxin-2 was co-expressed in HEK293T cells with a β-globin mini gene MS2bs reporter (FLAG-BGG(1–39)–MS2bs) containing eight contiguous copies of the MS2-binding site ( $8 \times$  MS2bs) in its 3'-UTR and a reference plasmid expressing 5×FLAG-enhanced GFP (EGFP) as the loading control, the length of the reporter mRNA increased markedly as compared with that in the GST control (Fig. 2 (A and B), compare lanes 1 and 2).

To determine whether the observed increase in mRNA length by the tethering of Ataxin-2 to the mRNA 3'-UTR was due to the extension of the poly(A) tail, the lengths of the reporter mRNAs that were treated with oligo(dT)/RNase H to remove the poly(A) tail were analyzed. This treatment produced a single band that migrated at the A0 (unpolyadenylated) position (Fig. 2 (D and E), compare lanes 1 and 2 with lanes 5 and 6, respectively). The results indicated that the observed increase of mRNA length was indeed due to the increased lengths of the poly(A) tails. The expression of Ataxin-2 protein was confirmed by Western blotting (Fig. 2F, lanes 1 and 2).

To further examine the possibility that Ataxin-2-induced poly(A) tail lengthening may be due to the binding of Ataxin-2 to PABPC1 through PAM2, we prepared Ataxin-2 with mutation at Phe-921 to alanine (F921A) in PAM2. The F921A



mutation abolished the binding of Ataxin-2 to PABPC1 (Fig. S1). Tethering of Ataxin-2 F921A to the 3'-UTR no longer increased the length of the reporter mRNA as compared with that in the GST control (Fig. 2 *A and B*, compare *lanes 1* and *3*). These results indicate that Ataxin-2 promotes lengthening of the poly(A) tail of the target mRNA through interaction with PABPC1. The expression of Ataxin-2 proteins was confirmed by Western blotting (Fig. 2*C*).

### Ataxin-2 specifically induces polyadenylation of the target mRNA

The observed increase in the length of the poly(A) tail could be explained by the two possible molecular events (*viz.* enhanced polyadenylation or inhibition of deadenylation). To distinguish these possibilities, we first determined whether the increase of poly(A) tail length that is mediated by Ataxin-2 could be caused by the inhibition of mRNA deadenylation by examining the effect of expressing catalytically inactive Pan2 and Caf1 mutants (Pan2 D1083A and Caf1 D161A, respectively) as described previously (35). The overexpression of these mutants completely inhibited deadenylation of the reporter mRNA in HEK293T cells (Fig. 2, *D*) (compare *lanes 1* and *3*) and *E*). Under these conditions, Ataxin-2 additionally increased the length of the mRNA poly(A) tail (Fig. 2, *D* (compare *lanes 3* and *4*) and *E*). This indicated that the Ataxin-2-induced increase in mRNA poly(A) tail length was not caused by the inhibition of mRNA deadenylation. Protein expression was confirmed by Western blotting (Fig. 2*F*). These results strongly suggest that Ataxin-2 extends mRNA poly(A) tail length via mRNA polyadenylation.

### Ataxin-2 C-terminal 906–1095 aa region containing PAM2 is necessary and sufficient for the polyadenylation of its target mRNA

The above result shows that PAM2 of Ataxin-2 is required for inducing polyadenylation of its target mRNA (Fig. 2, *A* and *B*); however, other regions may also be involved in the induction. Thus, we constructed a series of deletion mutants of Ataxin-2 to map the region required for the induction of polyadenylation. HEK293T cells were co-transfected with a reporter plasmid expressing FLAG-BGG(1–39)–MS2bs mRNA, a reference plasmid expressing 5×FLAG-EGFP as the loading control, and a plasmid expressing either MS2-fused 5×Myc-tagged GST, Ataxin-2, Ataxin-2(480–1313), Ataxin-2(549–1313), or Ataxin-2(906–1313) and with or without a plasmid

expressing HA-fused Pan2 D1083A and Caf1 D161A. All of the N-terminal deletion mutants tested (480–1313, 549–1313, and 906–1313) showed lengthening of the reporter mRNA to the same extent as WT Ataxin-2 when tethered to the mRNA. Moreover, the lengthening of the mRNA was again observed under conditions in which the deadenylase mutants (Pan2 D1083A and Caf1 D161A) were overexpressed (Fig. 3*A*, *lanes 6–10*). These results indicate that the C-terminal region 906–1313 containing PAM2 is important for the induction of polyadenylation (Fig. 3*G*). The expression of the WT and deletion mutant proteins was confirmed by Western blotting (Fig. 3*B*).

Additionally, a series of C-terminal deletion mutants were also examined. HEK293T cells were co-transfected with a reporter plasmid expressing FLAG-BGG(1–39)–MS2bs mRNA, a reference plasmid expressing 5×FLAG-EGFP as the loading control, and plasmid expressing either MS2-fused 5×Myc-tagged GST, Ataxin-2, Ataxin-2(906–1313), Ataxin-2(1–925), Ataxin-2(1–1005), Ataxin-2(1–1095), Ataxin-2(1–1140), or Ataxin-2(1–1223) and with or without a plasmid expressing HA-fused Pan2 D1083A and Caf1 D161A. The C-terminal deletion mutants (1–1223, 1–1140, and 1–1094) showed lengthening of the reporter mRNA, as was the case for Ataxin-2 WT (Fig. 3*C*, compare *lanes 1* and *2* with *lanes 6–8*), whereas 1–1005 and 1–925 showed no lengthening of the reporter mRNA as compared with that in the GST control (Fig. 3*C*, compare *lanes 1* and *2* with *lanes 4* and *5*). Moreover, the lengthening of the mRNA by the C-terminal deletion mutants (1–1223, 1–1140, and 1–1094) was again observed under conditions in which the deadenylase mutants Pan2 D1083A and Caf1 D161A were overexpressed (Fig. 3*C*, *lanes 9–16*). These results indicate that the 1006–1095 aa region is necessary for Ataxin-2-induced polyadenylation (Fig. 3*G*). Protein expression was confirmed by Western blotting (Fig. 3*D*).

Taken together, these results indicate that PAM2 as well as the region 1006–1095 is necessary for Ataxin-2-induced polyadenylation, suggesting that 906–1095 is sufficient for the induction of polyadenylation. To test this idea, we constructed Ataxin-2(906–1095) and examined its ability to induce polyadenylation of the reporter mRNA. As expected, Ataxin-2-induced polyadenylation was recapitulated by Ataxin-2(906–1095) (Fig. 3*E*). Protein expression was confirmed by Western blotting (Fig. 3*F*). Thus, Ataxin-2 C-terminal 906–1095 aa region containing PAM2 is necessary and sufficient for the polyadenylation of its target mRNA, suggesting that Ataxin-2 (906–1095) also enhances translation. As expected, tethering

**Figure 1. Ataxin-2 activates translation when tethered to a reporter mRNA.** *A*, schematic representations of the reporter constructs used for the MS2 tethering assay. *B*, HEK293T cells were co-transfected with the pcFLuc–MS2bs reporter plasmid, the pRLuc reference plasmid, and either pMS2-5×Myc-GST or pMS2-5×Myc-Ataxin-2. Firefly luciferase (*FLuc*) activity was measured and normalized to *Renilla* luciferase (*RLuc*) activity. The activity of pMS2-5×Myc-GST-transfected cells was defined as 1. Results were derived from three independent experiments and shown as the means ± S.D. (*error bars*). \*, *p* < 0.05. *C*, the amount of FLuc–MS2bs mRNAs was measured by real-time PCR. FLuc–MS2bs mRNA levels were normalized to those of RLuc mRNA. The mRNA level in pMS2-5×Myc-GST-transfected cells was defined as 1. Results were derived from three independent experiments and shown as the means ± S.D. \*, *p* < 0.05. *D*, the translation efficiency was calculated by normalization of protein level as in *B* to the corresponding mRNA level as in *C*. Results are means ± S.D. \*, *p* < 0.05. *E*, Western blotting (*WB*) to analyze the indicated protein expression. *F*, HEK293T cells were co-transfected with the pFLAG-CMV5/TO-BGG–MS2bs reporter plasmid and either pMS2-5×Myc-GST or pMS2-5×Myc-Ataxin-2 plasmid. After 48 h of plasmid transfection, the cells were lysed in buffer *B*. The cell lysates were fractionated by sucrose gradients. FLAG-BGG–MS2bs mRNA and GAPDH mRNA were analyzed by Northern blotting. *G*, the amount of FLAG-BGG–MS2bs mRNA and GAPDH mRNA in *F* was measured, in which the total amount of the mRNA was defined as 100%. Results were derived from three independent experiments and shown as the means ± S.D. *H*, the relative amounts of FLAG-BGG–MS2bs mRNA in nonpolysome (fractions 1–8), light polysome (fractions 9–12), and heavy polysome (fraction 13–15) that are isolated from pMS2-5×Myc-GST- or pMS2-5×Myc-Ataxin-2-transfected cells were measured. The mRNA level from pMS2-5×Myc-GST-transfected cells was defined as 1. Results were derived from three independent experiments and shown as the means ± S.D. \*, *p* < 0.05. *I*, the relative amounts of GAPDH mRNA were measured as in *H*.

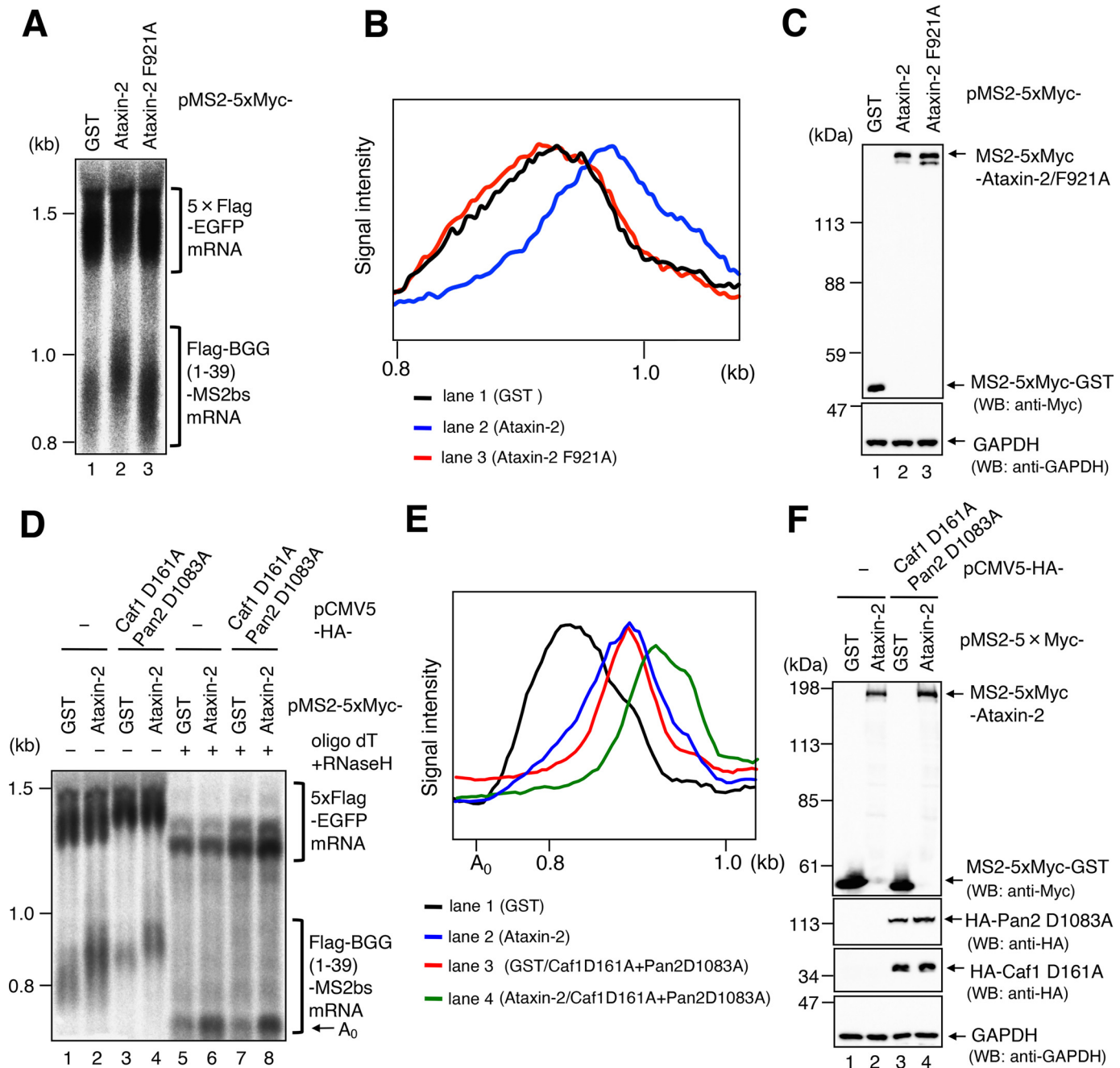
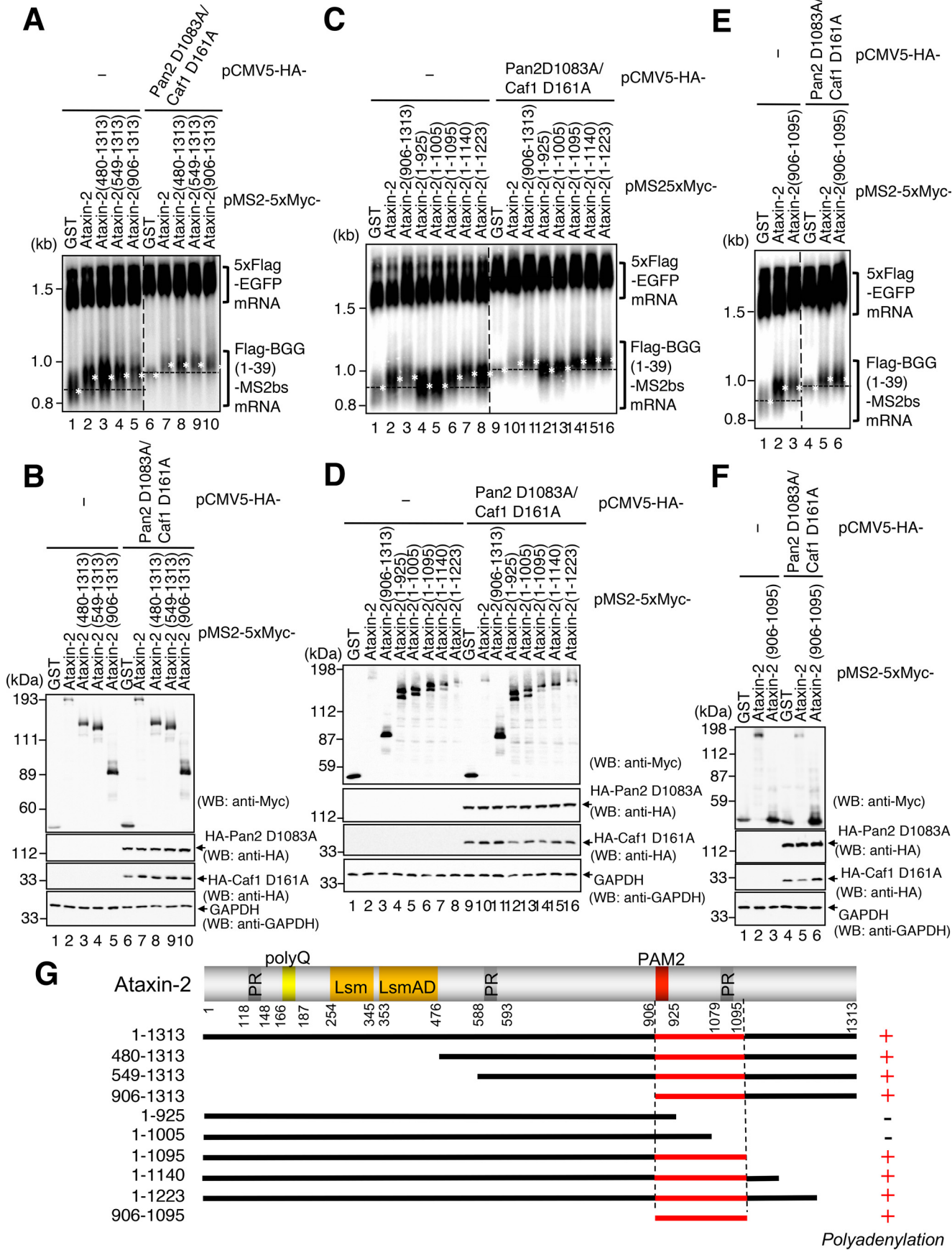


**Figure 2. Ataxin-2 extends poly(A) tail length of the target mRNA.** *A*, HEK293T cells were transfected with the pFLAG-CMV5/TO-BGG(1-39)-MS2bs reporter plasmid, pCMV-5×FLAG-EGFP reference plasmid, and either pMS2-5×Myc-GST, pMS2-5×Myc-Ataxin-2, or pMS2-5×Myc-Ataxin-2 F921A. Total RNA was isolated from each sample, and FLAG-BGG(1-39)-MS2bs mRNA and 5×FLAG-EGFP mRNA were detected by Northern blotting analysis. *B*, the length distribution (WB) of FLAG-BGG(1-39)-MS2bs mRNA in each lane of *A* was analyzed using Image Gauge version 4.23 (FUJIFILM) software. *C*, Western blotting (WB) to analyze the indicated protein expression. *D*, HEK293T cells were transfected with the pFLAG-CMV5/TO-BGG(1-39)-MS2bs reporter plasmid, pCMV-5×FLAG-EGFP reference plasmid, either pMS2-5×Myc-GST (*lanes 1, 3, 5*, and *7*) or pMS2-5×Myc-Ataxin-2 (*lanes 2, 4, 6*, and *8*), and either pCMV5-HA (*lanes 1, 2, 5*, and *6*) or pCMV5-HA-Caf1D161A plus pCMV5-HA-Pan2D1083A (*lanes 3, 4, 7*, and *8*). To produce deadenylated mRNA, each sample was treated with RNase H in the presence of oligo(dT) (*lanes 5-8*). The position of deadenylated (A<sub>0</sub>) FLAG-BGG(1-39)-MS2bs mRNA is indicated by an arrow. *E*, as in *B*, the length distribution of FLAG-BGG(1-39)-MS2bs mRNA in *lanes 1-4* of *D* was analyzed. *F*, Western blotting to analyze the indicated protein expression.

of Ataxin-2(906–1095) enhanced translation to a level comparable with that observed with Ataxin-2 (Fig. S3). From these results, we conclude that the 906–1095 aa region is necessary and sufficient not only for the induction of polyadenylation but also for enhancing translation of the target mRNA (Fig. 3*G*).

#### Ataxin-2 promotes post-transcriptional polyadenylation of target mRNAs

To precisely demonstrate that the observed poly(A) tail elongation is caused by the post-transcriptional polyadenylation, it is critical to exclude the possibility that Ataxin-2 promotes *de novo* synthesis of mRNA with a long poly(A) tail. Hence, we



monitored deadenylation kinetics of the Ataxin-2–tethered mRNA using a tetracycline-based pulse-chase assay as described previously (35). Considering that it is technically difficult to detect the pulse-induced reporter mRNA during a short period of time, we utilized Ataxin-2(480–1313) rather than full-length Ataxin-2 for this analysis as the reporter mRNA could easily be detectable in tethering experiments (Fig. 3A, compare *lanes* 2 and 3). After HEK293T-TREx cells were induced to express FLAG-BGG(1–39)–MS2bs mRNA by treatment of tetracycline, changes caused by deadenylation after transcriptional shut-off were analyzed. The results indicated that tethering Ataxin-2(480–1313) to the reporter mRNA decreased the rate of poly(A) tail shortening, as compared with that in the GST control (Fig. 4A, compare *lanes* 1–4 with *lanes* 5–8). Furthermore, under conditions in which the deadenylase mutants Pan2 D1083A and Caf1 D161A were overexpressed, deadenylation of the GST-tethered control mRNA was almost completely blocked (Fig. 4A, compare *lanes* 1–4 with *lanes* 9–12). In contrast, the poly(A) tail length of Ataxin-2(480–1313)–tethered mRNA showed a tendency to increase over time (Fig. 4A, *lanes* 13–16). However, it seems likely that the poly(A) tail had already elongated during the 2-h pulse time before the onset of chase analysis. Therefore, we next performed a tetracycline-based transcriptional turn-on analysis, in which changes in FLAG-BGG(1–39)–MS2bs mRNA poly(A) tail length were analyzed immediately after induction with tetracycline. In this case, we observed that the length of the poly(A) tail on Ataxin-2(480–1313)–tethered mRNA increased gradually under condition in which deadenylation of GST-tethered mRNA was completely inhibited by overexpressing deadenylase mutants (Fig. 4C, compare *lanes* 9–12 with *lanes* 13–16). Protein expression was confirmed by Western blotting (Fig. 4D). These results corroborate our conclusion that the Ataxin-2–induced increase in mRNA poly(A) tail length was due to the polyadenylation of the pre-existing mRNA but not due to the inhibition of mRNA deadenylation.

#### Ataxin-2 specifically binds to PAPD4 to induce polyadenylation of a target mRNA

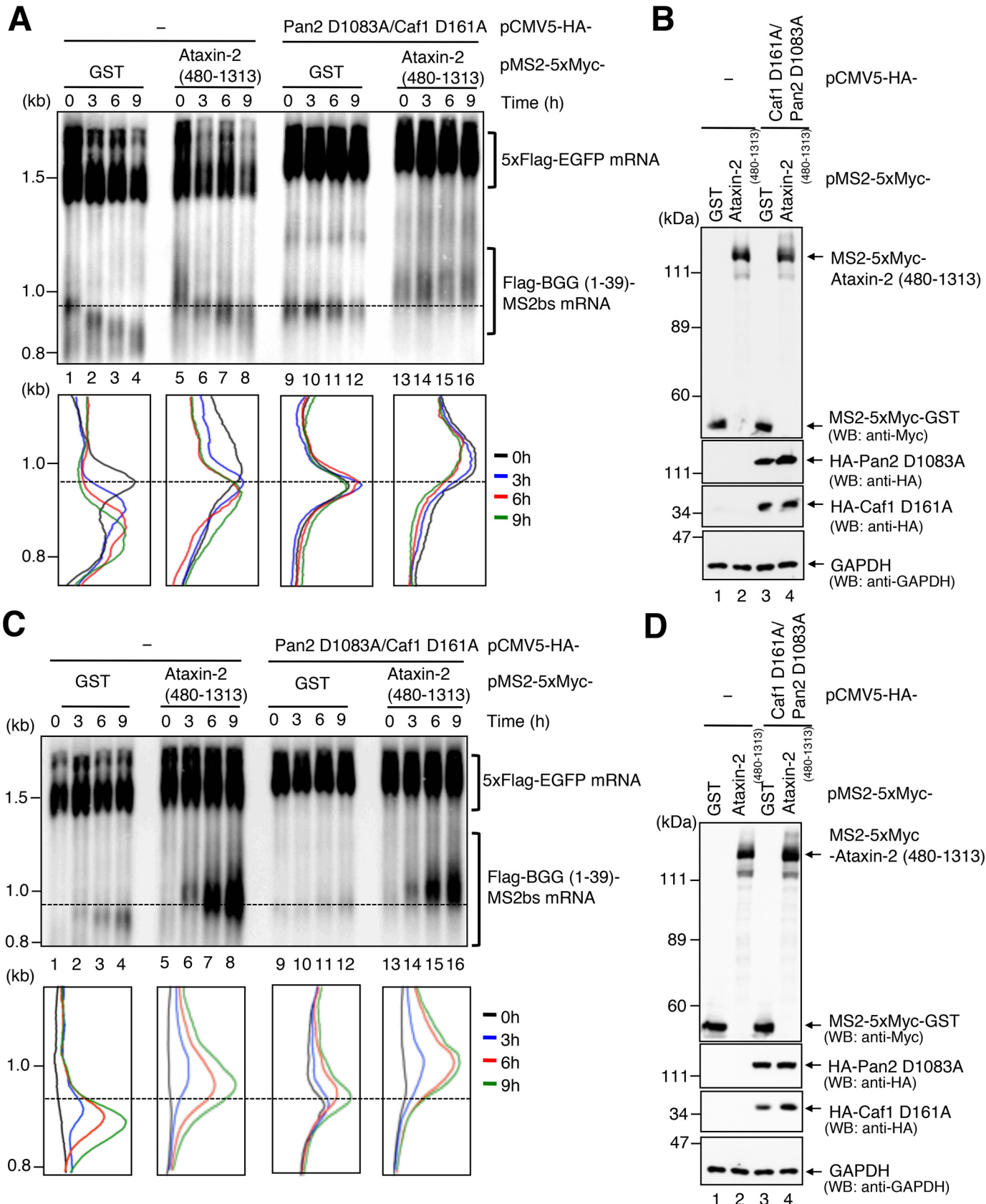
Cytoplasmic polyadenylation can be executed post-transcriptionally by noncanonical poly(A) polymerase (46, 47). Based on the above results, it is reasonable to hypothesize that Ataxin-2 induces mRNA polyadenylation through an interaction with one of these enzymes. To test this idea, interaction between Ataxin-2 and noncanonical poly(A) polymerases was examined using an immunoprecipitation assay. HEK293T cells

were co-transfected with a plasmid expressing 5×FLAG-Ataxin-2 and a plasmid expressing 5×Myc-tagged PAPD3, PAPD4, PAPD5, PAPD6, or PAPD7. Cell extracts were prepared and subjected to immunoprecipitation with an anti-FLAG antibody. The most prominent interaction was observed between 5×FLAG-Ataxin-2 and 5×Myc-PAPD4, whereas 5×FLAG-Ataxin-2 also co-precipitated with a trace amount of the other 5×Myc-PAPDs (Fig. 5, A–E). The results indicate that Ataxin-2 preferentially binds to PAPD4 over other noncanonical poly(A) polymerases. The observed interactions do not appear to be mediated by RNA, as all of the immunoprecipitation experiments in this study were performed under buffer conditions that include RNase I. The interaction between endogenous Ataxin-2 and PAPD4 was further confirmed with endogenous proteins. HEK293T cell lysate was subjected to immunoprecipitation using anti-PAPD4 antibody. Endogenous PAPD4 co-precipitated with endogenous Ataxin-2 (Fig. 5F).

Based on our finding that the Ataxin-2(906–1095) region is necessary and sufficient for Ataxin-2–induced polyadenylation, we anticipated that the Ataxin-2(906–1095) region interacts with PAPD4. To test this idea, we performed an immunoprecipitation assay. HEK293T cells were co-transfected with a plasmid expressing either 5×FLAG-Ataxin-2 or 5×FLAG-Ataxin-2(906–1095) and a plasmid expressing 5×Myc-PAPD4. Cell extracts were prepared and subjected to immunoprecipitation with an anti-FLAG antibody. Consistent with the expectation, 5×Myc-PAPD4 co-precipitated with 5×FLAG-Ataxin-2 (906–1095) as well as 5×FLAG-Ataxin-2 (Fig. 5G).

These results strongly suggest that PAPD4 mediates Ataxin-2–induced polyadenylation. To confirm this, we utilized an RNAi-mediated knockdown strategy. HEK293T cells were co-transfected with the following: a reporter plasmid expressing FLAG-BGG(1–39)–MS2bs mRNA, reference plasmid expressing 5×FLAG-EGFP as the transfection/loading control, and a plasmid expressing either MS2-fused 5×Myc-tagged Ataxin-2 or GST and either PAPD4 siRNA or control siRNA. The results indicated that PAPD4 siRNA down-regulated PAPD4 protein levels to 49% (Fig. 6C). Under this condition, the partial down-regulation led to the partial repression of Ataxin-2–induced polyadenylation without affecting the GST control (Fig. 6, A and B). On the other hand, knockdown of either PAPD3, PAPD5, PAPD6, or PAPD7 had no effect on Ataxin-2–induced polyadenylation (Fig. S4). These results provide convincing evidence that PAPD4 mediates Ataxin-2–induced mRNA polyadenylation.

**Figure 3. The C-terminal 906–1095 aa region is necessary and sufficient for the induction of the poly(A) tail lengthening of target mRNAs.** A, HEK293T cells were co-transfected with the pFLAG-CMV5/TO-BGG(1–39)–MS2bs reporter plasmid, pCMV-5×FLAG-EGFP reference plasmid, and a combination of either pMS2-5×Myc-GST (*lanes* 1 and 6), pMS2-5×Myc-Ataxin-2 (*lanes* 2 and 7), pMS2-5×Myc-Ataxin-2(480–1313) (*lanes* 3 and 8), pMS2-5×Myc-Ataxin-2(549–1313) (*lanes* 4 and 9) or pMS2-5×Myc-Ataxin-2(906–1313) (*lanes* 5 and 10), and either pCMV5-HA (*lanes* 1–5) or pCMV5-HA-Caf1 D161A plus pCMV5-HA-Pan2 D1083A (*lanes* 6–10). B, Western blotting (WB) to analyze the indicated protein expression. C, HEK293T cells were co-transfected with the pFLAG-CMV5/TO-BGG(1–39)–MS2bs reporter plasmid, pCMV-5×FLAG-EGFP reference plasmid, and a combination of either pMS2-5×Myc-GST (*lanes* 1 and 9), pMS2-5×Myc-Ataxin-2 (*lanes* 2 and 10), pMS2-5×Myc-Ataxin-2(906–1313) (*lanes* 3 and 11), pMS2-5×Myc-Ataxin-2(1–925) (*lanes* 4 and 12), pMS2-5×Myc-Ataxin-2(1–1005) (*lanes* 5 and 13), pMS2-5×Myc-Ataxin-2(1–1095) (*lanes* 6 and 14), pMS2-5×Myc-Ataxin-2(1–1140) (*lanes* 7 and 15), or pMS2-5×Myc-Ataxin-2(1–1223) (*lanes* 8 and 16) and either pCMV5-HA (*lanes* 1–8) or pCMV5-HA-Caf1 D161A plus pCMV5-HA-Pan2 D1083A (*lanes* 9–16). D, Western blotting to analyze the indicated protein expression. E, HEK293T cells were co-transfected with the pFLAG-CMV5/TO-BGG(1–39)–MS2bs reporter plasmid, pCMV-5×FLAG-EGFP reference plasmid, and a combination of either pMS2-5×Myc-GST (*lanes* 1 and 4), pMS2-5×Myc-Ataxin-2 (*lanes* 2 and 5), or pMS2-5×Myc-Ataxin-2(906–1095) (*lanes* 3 and 6) and either pCMV5-HA (*lanes* 1–3) or pCMV5-HA-Caf1 D161A plus pCMV5-HA-Pan2 D1083A (*lanes* 4–6). F, Western blotting to analyze the indicated protein expression. G, schematic diagram of MS2-5×Myc-Ataxin-2 fragments with a summary of the Ataxin-2–induced polyadenylation results. PR, proline-rich domain; LSm, LSm domain; LSmAD, LSm-associated domain; PAM2, PABPC1-interacting motif 2.



### Ataxin-2 and PAPD4 regulate polyadenylation of cyclin D1 and TDP-43 mRNAs

A previous study has demonstrated that Ataxin-2 regulates the expression of targets, including cyclin D1 and TDP-43 mRNAs, by binding to their 3'-UTR (44). To determine whether Ataxin-2 and PAPD4 regulate the poly(A) tail length of endogenous cyclin D1 and TDP-43 mRNAs, HEK293T cells were transfected with siRNA against either Ataxin-2, PAPD4, or luciferase (control), and the poly(A) tail length of cyclin D1 and TDP-43 mRNAs was analyzed using an RNA ligation-mediated poly(A) test (RL-PAT) assay. The poly(A) tail length of cyclin D1 and TDP-43 mRNAs was decreased by the knockdown of Ataxin-2 and PAPD4, whereas the poly(A) tail length of GAPDH mRNA, which does not contain the Ataxin-2 target sequence, was not affected (Fig. 7, A and B). The rate of cyclin D1 mRNAs with short poly(A) tails was significantly increased 2.2- and 3.1-fold by the knockdown of Ataxin-2 and PAPD4, respectively (Fig. 7C, left), and that of TDP-43 mRNAs was also increased 1.3- and 1.4-fold by the knockdown of Ataxin-2 and PAPD4, respectively (Fig. 7C, middle). No changes were observed for the control GAPDH mRNA (Fig. 7C, right). The expression of Ataxin-2 and PAPD4 proteins was confirmed by Western blotting (Fig. 7D).

To test the effect of Ataxin-2 and PAPD4 knockdown on translation of cyclin D1 and TDP-43 mRNAs, we analyzed the corresponding proteins by Western blotting. The results indicated that the cyclin D1 and TDP-43 protein levels decreased to 60 and 81%, respectively, by knockdown of Ataxin-2 and decreased to a similar degree (53 and 75%, respectively) by knockdown of PAPD4 (Fig. 7, D and E). These results are consistent with the notion that Ataxin-2, in complex with PAPD4, induces polyadenylation of its target mRNAs to positively regulate its gene expression.

### Discussion

Several studies have suggested that Ataxin-2 is implicated in translational control. In *Caenorhabditis elegans*, ATX-2, the ortholog of Ataxin-2, forms a complex with the cytoplasmic poly(A)-binding protein PAB-1 and functions in germline formation, which is known to require translation (48). *Drosophila* Ataxin-2, ATX2, also forms a complex with PABP and is involved in translation-dependent long-term memory (49). Moreover, ATX2 acts as a circadian pacemaker by mediating the interaction of translation activator TWENTY-FOUR (TYF) with PABP and regulates expression of the rate-limiting clock component PERIOD (PER) (50, 51). In mammals, Ataxin-2 associates with the pre-initiation complex, and genetic ablation

of Ataxin-2 leads to increased expression of ribosomal proteins and translation initiation factors as well as phosphorylation of ribosomal protein S6 and translation factor 4EBP through the phosphoinositide 3-kinase-mTOR pathway (52). These results suggest that Ataxin-2 might be a translation regulator conserved among higher eukaryotes. Here, we provide direct evidence showing that Ataxin-2 enhances translation of the target mRNA and further provide a mechanistic basis for the Ataxin-2-induced translation activation; Ataxin-2 binds to PABPC1 and PAPD4 via the PAM2-containing intrinsically disordered region (906–1095 aa) and recruits PAPD4 to the target mRNA to induce post-transcriptional polyadenylation, thereby activating translation (see Fig. 7F). It is therefore tempting to speculate that Ataxin-2 regulates translation of specified targets during germline formation, long-term habituation, and circadian rhythm formation by using the mechanism proposed in this study. In this context, it is noteworthy that, in *Drosophila*, both Gld2 poly(A) polymerase, an ortholog of PAPD4, and ATX2 are required for long-term but not short-term memory (53).

It is now widely accepted that RNA-binding proteins negatively regulate gene expression through accelerated deadenylation of target mRNAs. The most extensively investigated example is the RNA-binding protein TTP, which directly binds to AREs and recruits the Ccr4–Not complex to accelerate deadenylation and decay of target mRNAs (18, 19). In a similar manner, CPE-binding proteins (CPEB and CPEB3) (20, 21), Smaug (22), PUF (23), Roquin (24), hnRNPA1 (25), CUGBP1 (26), RBPMS (27), TDP-43 (28), and microRNA RISC (29–31) regulate gene expression of the target mRNAs through deadenylation. Therefore, negative regulation by deadenylation is recognized as a widespread and effective means to regulate gene expression. In sharp contrast, positive regulation through polyadenylation has been most extensively studied in the context of early development (32). In oocyte maturation and embryogenesis, CPEB facilitates the cytoplasmic polyadenylation of maternal mRNA by PAPD4 to promote translation (53, 54). However, cytoplasmic polyadenylation is not well-established in somatic cells. The main reason for this is that in contrast to early development, where transcription is ceased and gene expression is absolutely dependent on deadenylation and polyadenylation of the maternal mRNAs, somatic cells actively perform RNA synthesis, translation, and turnover. To overcome this, we have developed a method to enable specific detection of cytoplasmic polyadenylation by performing transcriptional pulse-chase analysis under conditions where deadenylases are suppressed (35). Using this strategy, we have demonstrated that a member of the STAR family of RNA-binding proteins, QKI, plays a role

**Figure 4. Ataxin-2 induces post-transcriptional polyadenylation of target mRNAs.** A, HEK293T-TREx cells were co-transfected with the pFLAG-CMV5/TO-BGG(1–39)–MS2bs reporter plasmid, pCMV-5×FLAG-EGFP reference plasmid, pT7-TR plasmid, and a combination of either pMS2-5×Myc-GST (lanes 1–4 and 9–12) or pMS2-5×Myc-Ataxin-2(480–1313) (lanes 5–8 and 13–16) and either pCMV5-HA (lanes 1–8) or pCMV5-HA-Caf1 D161A plus pCMV5-HA-Pan2 D1083A (lanes 9–16). One day after the transfection, FLAG-BGG(1–39)–MS2bs mRNA was induced for 2 h by tetracycline treatment. FLAG-BGG(1–39)–MS2bs mRNA was analyzed at the specified time after the induction. Top, FLAG-BGG(1–39)–MS2bs mRNA was detected by Northern blotting. Bottom, as in Fig. 2B, FLAG-BGG(1–39)–MS2bs mRNA length distribution was analyzed. B, Western blotting (WB) to analyze the indicated protein expression. C, HEK293T-TREx cells were co-transfected with the pFLAG-CMV5/TO-BGG(1–39)–MS2bs reporter plasmid, the pCMV-5×FLAG-EGFP reference plasmid, the pT7-TR plasmid, and a combination of either pMS2-5×Myc-GST (lanes 1–4 and 9–12) or pMS2-5×Myc-Ataxin-2(480–1313) (lanes 5–8 and 13–16) and either pCMV5-HA (lanes 1–8) or pCMV5-HA-Caf1 D161A plus pCMV5-HA-Pan2 D1083A (lanes 9–16). One day after the transfection, FLAG-BGG(1–39)–MS2bs mRNA was induced by tetracycline treatment. FLAG-BGG(1–39)–MS2bs mRNA at the specified time after the induction was analyzed. Top, FLAG-BGG(1–39)–MS2bs mRNA was detected by Northern blotting. Bottom, as in Fig. 2B, FLAG-BGG(1–39)–MS2bs mRNA length distribution was analyzed. D, Western blotting to analyze the indicated protein expression.

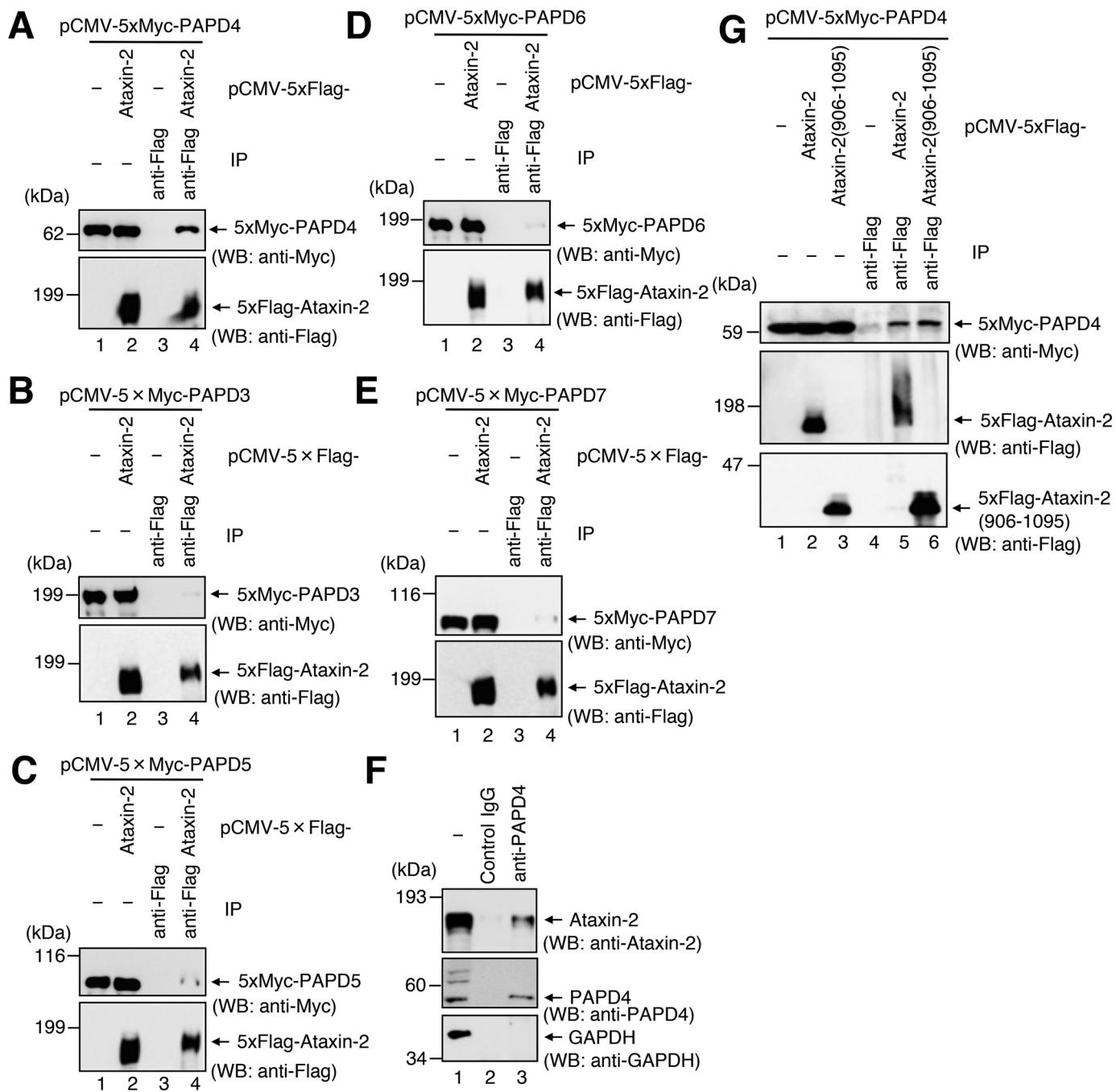


**Figure 5. Ataxin-2 specifically interacts with PAPD4.** *A*, HEK293T cells were transfected with pCMV-5×Myc-PAPD4 and either pCMV-5×FLAG (lanes 1 and 3) or pCMV-5×FLAG-Ataxin-2 (lanes 2 and 4). IP analysis using anti-FLAG antibody was performed. The immunoprecipitates (lanes 3 and 4) and inputs (lanes 1 and 2) were analyzed by Western blotting (WB) using the indicated antibodies. *B*, as in *A*, except that pCMV-5×Myc-PAPD3 was used instead of pCMV-5×Myc-PAPD4. *C*, as in *A*, except that pCMV-5×Myc-PAPD5 was used instead of pCMV-5×Myc-PAPD4. *D*, as in *A*, except that pCMV-5×Myc-PAPD6 was used instead of pCMV-5×Myc-PAPD4. *E*, as in *A*, except that pCMV-5×Myc-PAPD7 was used instead of pCMV-5×Myc-PAPD4. *F*, IP analysis using anti-PAPD4 or normal goat IgG as the nonspecific control was performed. The immunoprecipitates (lanes 2 and 3) and input (lane 1) were analyzed by Western blotting using the indicated antibodies. *G*, HEK293T cells were transfected with pCMV-5×Myc-PAPD4 and either pCMV-5×FLAG (lanes 1 and 4), pCMV-5×FLAG-Ataxin-2 (lanes 2 and 5), or pCMV-5×FLAG-Ataxin-2(906–1095) (lanes 3 and 6). IP analysis using anti-FLAG antibody was performed. The immunoprecipitates (lanes 4–6) and inputs (lanes 1–3) were analyzed by Western blotting using the indicated antibodies.

in cytoplasmic polyadenylation in somatic cells. The cytoplasmic isoform of QKI (QKI-7) binds to the target mRNAs (hnRNPA1, p27<sup>kip1</sup>, and β-catenin) in a manner dependent on the QKI response element to recruit PAPD4, thereby eliciting polyadenylation and translation activation of the targets (35). By discovering the third example of the cytoplasmic poly-

adenylation specificity factor, Ataxin-2, it is now possible to delineate a generalized model for the mechanism of positive regulation of gene expression by cytoplasmic polyadenylation. Cytoplasmic polyadenylation specificity factor, which binds to the cis-element in the 3'-UTR of target mRNA, recruits a non-canonical poly(A) polymerase (*i.e.* PAPD4) to the mRNA to

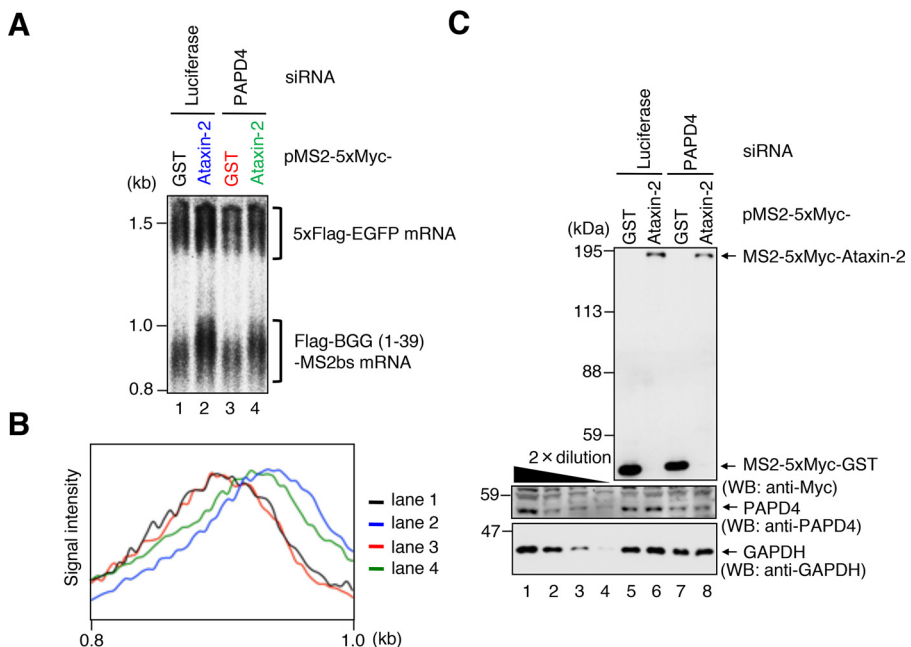


**Figure 6. PAPD4 mediates Ataxin-2-induced polyadenylation of mRNA.** *A*, HEK293T cells were transfected with either luciferase siRNA (*lanes 1* and *2*) or PAPD4 siRNA (*lanes 3* and *4*), the pFLAG-CMV5/TOBGG(1–39)–MS2bs reporter plasmid, pCMV-5×FLAG-EGFP reference plasmid, and either pMS2-5×Myc-GST (*lanes 1* and *3*) or pMS2-5×Myc-Ataxin-2 (*lanes 2* and *4*). FLAG-BGG(1–39)–MS2bs mRNA and 5×FLAG-EGFP mRNA were analyzed by Northern blotting. *B*, as in Fig. 2*B*, FLAG-BGG(1–39)–MS2bs mRNA length distribution of *A* was analyzed. *C*, Western blotting (WB) to analyze the indicated protein expression.

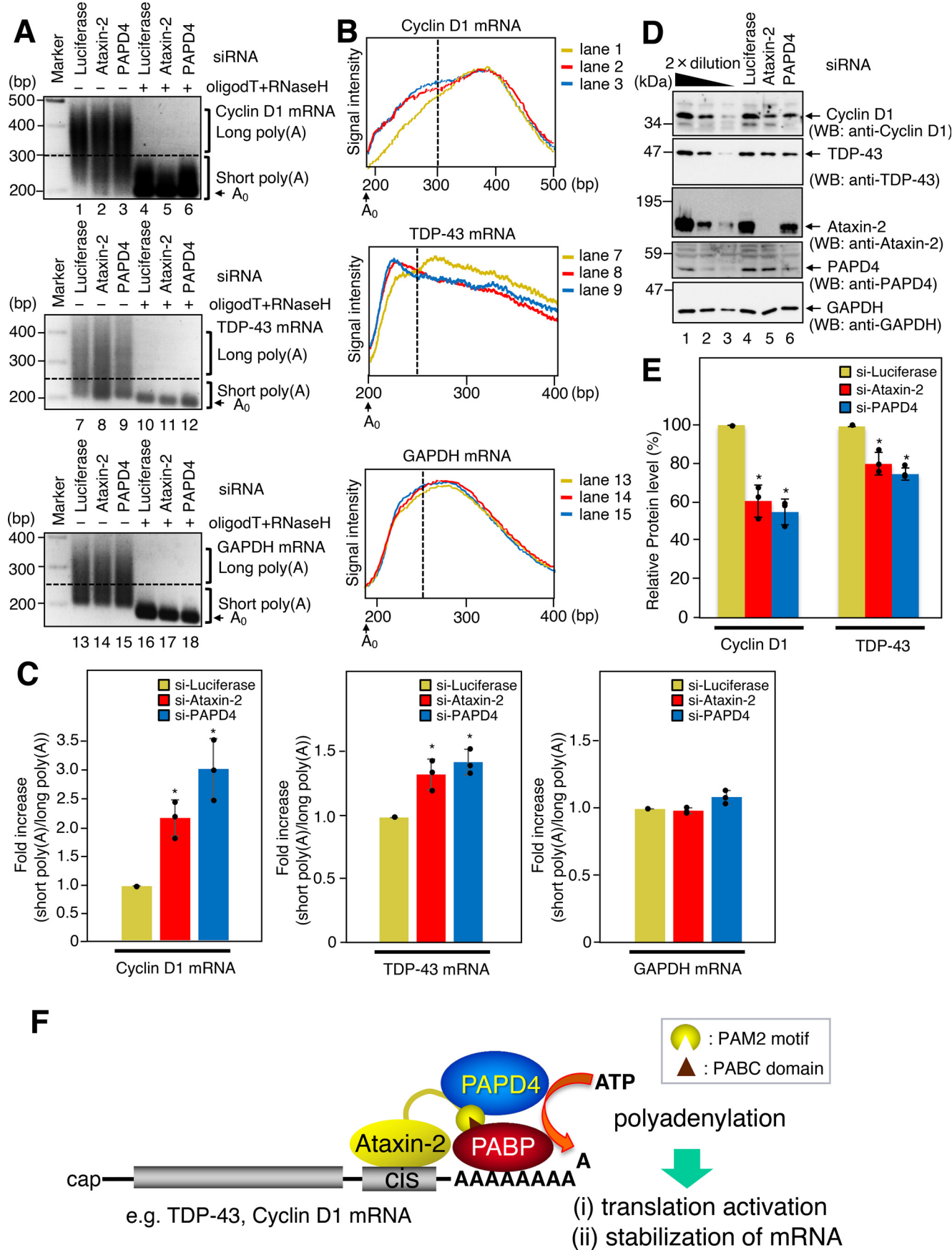
elicit elongation of the poly(A) tail, thereby activating translation. mRNA 3' poly(A) tails are covered with the general RNA-binding protein PABPC1. PABPC1 is thus a key player in mRNA poly(A) tail metabolism (4). Studies by us and others have demonstrated that PAM2 motif-containing proteins, which bind specifically to PABPC1, are involved in mRNA poly(A) tail metabolism (10, 13, 55). Antiproliferative protein Tob and Pan3 bind to the catalytic subunits of Caf1 and Pan2 deadenylases, respectively, and recruit them to PABPC1 bound to the poly(A) tail via PAM2, which leads to the deadenylation of the mRNAs (10, 13, 55). The eukaryotic releasing factor eRF3 also contains PAM2 in the N-terminal intrinsically disordered region and binds to PABPC1 (10). This binding is required for efficient termination and the termination-coupled deadenylation of mRNAs (10). In the present study, we further showed that PAM2 is also involved in the post-transcriptional polyadenylation of mRNAs. In addition to the direct recognition of the cis-regulatory AU-rich elements by the RNA-binding LSM domain, Ataxin-2 indirectly recognizes the poly(A) tail through PAM2-mediated contact with PABPC1, which is assumed to increase the binding specificity of Ataxin-2 to the cis-element close to the polyadenylation site of the mRNA and enables the recruitment of PAPD4 to the polyadenylation site.

In conclusion, our work demonstrates that Ataxin-2 induces cytoplasmic polyadenylation to enhance translation of the targets, including TDP-43 mRNA. An intriguing hypothesis is that Ataxin-2 not only plays physiological roles in regulating germline formation, long-term habituation, and circadian rhythm formation but also modifies neurodegeneration (*i.e.* TDP-43 proteinopathies) through translational regulation of the target mRNAs. Further investigations are needed to elucidate these possibilities.

## Experimental procedures

### Plasmids

The N terminus of Ataxin-2 cDNA was obtained from HeLa reverse transcriptase (RT) products as the template. Ataxin-2 (1–79) and Ataxin-2(71–458) were PCR-amplified using the primer pairs NH116/NH266 and NH258/NH262, respectively. Ataxin-2(1–458) was generated by In-Fusion PCR using Ataxin-2(1–79) and Ataxin-2(71–458) as the template. The C terminus of Ataxin-2 cDNA was obtained from BC111757 (IMAGE clone cDNA). To construct pCMV-5×FLAG-Ataxin-2, Ataxin-2(459–1313) was PCR-amplified using the primer pair NH112/NH113. Ataxin-2(1–458) fragment was digested with HindIII and XhoI, and Ataxin-2(459–1313) fragment was digested with XhoI and Sall and inserted into the HindIII and Sall sites of pCMV-5×FLAG (56). To construct pCMV-5×Myc-Ataxin-2, pCMV-5×FLAG-Ataxin-2 was digested with HindIII and Sall, and the Ataxin-2 cDNA fragment was inserted into the HindIII and Sall sites of pCMV-5×Myc (20). To construct pMS2-5×Myc-Ataxin-2, the ORF of Ataxin-2 was PCR-amplified using the primer pair NH540/CMV6 and pCMV-5×FLAG-Ataxin-2 as the template. The resulting fragment was digested with SalI and inserted into the EcoRV and XhoI sites of pMS2-5×Myc (35). pMS2-5×Myc-Ataxin-2 F921A was generated by inverse PCR using pMS2-5×Myc-Ataxin-2 and the primer pair NH134/NH135. To generate pMS2-5×Myc-Ataxin-2(480–1313), pMS2-5×Myc-Ataxin-2(549–1313), pMS2-5×Myc-Ataxin-2(906–1313), pMS2-5×Myc-Ataxin-2(1–925), pMS2-5×Myc-Ataxin-2(1–1005), pMS2-5×Myc-Ataxin-2(1–1095), pMS2-5×Myc-Ataxin-2(1–1140), pMS2-5×Myc-Ataxin-2(1–1223), and pMS2-5×Myc-Ataxin-2(906–1095), the corresponding cDNA fragments of Ataxin-2 were PCR-amplified using the primer



pairs HI003/NH113, ry136/NH113, ry137/NH113, NH114/NH1063, NH114/HT019, NH114/HT015, NH114/HT016, NH114/HT017, and ry137/HT015, respectively, and pMS2-5×Myc-Ataxin-2 as the template. The resulting fragments were digested with SalI and inserted into the EcoRV and XhoI sites of pMS2-5×Myc. To construct pCMV-5×FLAG-Ataxin-2(906-1095), Ataxin-2(906-1095) was subjected to PCR using the primer pair HT020/HT015 and pCMV-5×FLAG-Ataxin-2 as the template. Ataxin-2(906-1095) fragment was digested with EcoRI and SalI and inserted into the EcoRI and SalI sites of pCMV-5×FLAG. To construct pCMV-5×Myc-PAPD3, the ORF of PAPD3 was PCR-amplified using the primer pair NH897/NH898 and HeLa RT products as the template. The resulting fragment was digested with EcoRI and XhoI and inserted into pCMV-5×Myc. To construct pCMV-5×Myc-PAPD6, the ORF of PAPD6 was subjected to PCR using the primer pair NH899/NH900 and HeLa RT product as the template. The resulting fragment was digested with EcoRI and XhoI and inserted into pCMV-5×Myc. pAAVS1-Puro was generated by inverse PCR using AAVS1\_Puro\_PGK1\_3×FLAG\_Twin\_Strep (Addgene) and the primer pair RS018/RS019. To construct pAAVS1-Puro-CMV-T7-TR, CMV-T7-TR was PCR-amplified using the primer pair RS016/RS017 and pT7-TR as the template. The resulting fragment was digested with SalI and inserted into the EcoRV and SalI sites of pAAVS1-Puro. The construction of all other plasmids used in this study was described previously (20, 35, 57). The synthetic oligonucleotides used in this study are listed in Table S1.

### siRNA

Ataxin-2, PAPD4, and luciferase siRNA consisted of 5'-r(CUU ACA GUC CGA AGU GUG A)d(TT)-3', 5'-r(CUU AUG CAU ACC UUG AAA A)d(TT)-3', and 5'-r(CGU ACG CGG AAU ACU UCG A)d(TT)-3', respectively.

### Cell lines

HEK293T cells were cultured in Dulbecco's modified Eagle's medium (Nissui) supplemented with 5% fetal bovine serum, and maintained at 37 °C in 5% CO<sub>2</sub>. HEK293T-TREx cells were obtained by transfection of pAAVS1-Puro-CMV-T7-TR, gRNA\_AAVS1-T2 (Addgene), and hCas9 (Addgene), followed by 2.0 µg/ml puromycin selection.

### DNA/RNA transfection

Plasmid DNA transfection was performed using Polyethyleneimine Max (Polyscience, Inc.) or Lipofectamine 3000 (Invitrogen). For siRNA transfection, Lipofectamine RNAiMAX (Invitro-

gen) was used. For co-transfection with both siRNA and plasmid DNA, Lipofectamine 2000 (Invitrogen) was used.

### Antibodies

The antibodies used in this study were anti-Myc (9E10 (Roche), A-14 (Santa Cruz Biotechnology, Inc.), or My3 (MBL)), anti-HA (3F10, Roche), anti-FLAG (M2, Sigma), anti-Ataxin-2 (BD Transduction Laboratories or raised against His-tagged Ataxin-2(480-907) protein), anti-cyclin D1 (H-295, Santa Cruz Biotechnology), anti-PAPD4<sup>1</sup> (N-15, Santa Cruz Biotechnology), anti-PAPD4<sup>2</sup> (raised against His-tagged PAPD4 (1-141) protein and His-tagged PAPD4(1-182) protein), anti-GAPDH (raised against His-tagged GAPDH protein), and anti-TDP-43 (raised against His-tagged TDP-43 protein), respectively.

### Immunoprecipitation

The transfected cells were lysed in buffer A (20 mM Tris-HCl (pH 7.5), 50 mM NaCl, 2.5 mM EDTA, 0.5% Nonidet P-40, 1 mM DTT, 0.1 M phenylmethylsulfonyl fluoride, 2 µg/ml aprotinin, 2 µg/ml leupeptin, and 2 µg/ml pepstatin A) at 4 °C for 10 min. The supernatant by centrifugation at 15,000 rpm for 10 min at 4 °C was incubated with anti-FLAG IgG-agarose (Sigma) and 50 units/ml RNase I (New England Biolabs) for 1 h at 10 °C. Following washing of the agarose resin using buffer A, the bound protein was eluted with SDS-PAGE sample buffer and analyzed by Western blotting. For an immunoprecipitation (IP) assay using anti-PAPD4<sup>1</sup> antibody to detect endogenous interactions, the lysate isolated from nontransfected cells was incubated with either anti-PAPD4<sup>1</sup> antibody or normal goat IgG (Santa Cruz Biotechnology) and Protein G-Sepharose 4 Fast Flow (GE Healthcare) and subjected to immunoprecipitation. PAPD4 protein was detected with anti-PAPD4<sup>2</sup> antibody.

### Northern blotting analysis

Total RNA isolation and RNase H treatment of mRNA to generate deadenylated (A<sub>0</sub>) mRNA were performed as described previously (35). HEK293T-TREx cells, which express the T7-tagged tetracycline receptor, a reporter plasmid, and the specified plasmids, were subjected to transcriptional turn-on analysis and pulse-chase analysis. After 24 h of transfection, cells were treated with 40 ng/ml tetracycline to induce transcription. For transcriptional turn-on analysis, cells were harvested at the specified times after transcription start. For transcriptional pulse-chase analysis, cells were treated with tetracycline for 2 h to induce transcription and were harvested at the specified times after transcription shut-off. Total RNA was analyzed by Northern blotting using either <sup>33</sup>P-labeled nucleotides or digoxigenin (DIG)-labeled RNA probe. FLAG-BGG(1-

**Figure 7. Ataxin-2 and PAPD4 regulate poly(A) tail length of endogenous target mRNAs of Ataxin-2.** A, HEK293T cells were transfected with either luciferase, Ataxin-2, or PAPD4 siRNA. The RL-PAT assay was performed to investigate the poly(A) tail length of the endogenous cyclin D1, TDP-43, and GAPDH mRNAs. B, as in Fig. 2B, the poly(A) tail length distribution of the endogenous cyclin D1, TDP-43, and GAPDH mRNAs of A was analyzed. C, the amount of mRNA with a short poly(A) tail was measured and normalized to mRNA with a long poly(A) tail. The levels in luciferase siRNA-transfected cells were defined as 1. Results were representative of three independently performed experiments and shown as the means ± S.D. (error bars). \*, p < 0.05. D, Western blotting (WB) to analyze the indicated protein expression. E, the expression levels of cyclin D1 and TDP-43 proteins were calculated and normalized to that of GAPDH protein. The levels in luciferase siRNA-transfected cells were defined as 100%. Results were representative of three independently performed experiments and shown as the means ± S.D. \*, p < 0.05. F, model for the post-transcriptional polyadenylation and translation activation by Ataxin-2.

39)-MS2bs and 5×FLAG-EGFP mRNAs were detected using  $^{33}\text{P}$ -labeled nucleotides (NH208/NH264/NH265). To detect GAPDH, 5×FLAG-EGFP, FLAG-BGG-MS2bs, and FLAG-BGG(1-39)-MS2bs mRNAs using a DIG-labeled RNA probe, the ORFs of GAPDH, EGFP, and BGG and BGG(1-39)-MS2bs fragment were inserted into pBluescriptII-SK(−). The generated pBluescriptII-SK(−) plasmids were linearized, and the DIG-labeled RNA probe was synthesized using T7 RNA polymerase in the presence of DIG-11-UTP according to the manufacturer's instructions (Roche).

#### RL-PAT assay

RL-PAT assay was performed as described previously (35). In brief, 2  $\mu\text{g}$  of total RNA was ligated to 50 pmol of anchor primer KO146 using T4 RNA ligase 1 (New England Biolabs). The ligated RNA was subjected to the reverse transcriptase reaction, using primer NH20 and SuperScript III reverse transcriptase (Invitrogen) according to the manufacturer's instructions. After the gene-specific poly(A) tail region was amplified by semi-nested PCR using the gene-specific sense primers and anchor antisense primer KO197, the resulting fragments were separated on 2% agarose gel and detected by ethidium bromide staining. The poly(A) tail of cyclin D1 mRNA was detected using the primer pair HI010/KO197 in the first PCR and the primer pair HI015/KO197 in the second PCR. That of TDP-43 mRNA was amplified using the primer pair HI014/KO197 in the first PCR and the primer pair HI016/KO197 in the second PCR. That of GAPDH mRNA was detected using primer pair ry-104/KO197 in the first PCR and primer pair ry-105/KO197 in the second PCR.

#### Luciferase assay

After 48 h of transfection, HEK293T cells were lysed and assayed by using the Dual-Glo Luciferase Assay system (Promega) following the manufacturer's protocol.

#### Quantitative real-time PCR

Total RNA was isolated, and genomic DNA was removed by digestion with DNase I. Reverse transcriptase reactions were performed using MultiScribe reverse transcriptase (Thermo Fisher Scientific) with gene-specific primers. Firefly luciferase and *Renilla* luciferase mRNAs were reverse-transcribed with HI035 and HI039, respectively. Real-time PCR analysis was performed using the 7300 Real-Time PCR system with Power SYBR Green PCR Master Mix (Applied Biosystems). Firefly luciferase and *Renilla* luciferase mRNAs were amplified using HI034/HI035 and HI038/HI039, respectively.

#### Polysome profile analysis

Polysome profile analysis by sucrose density gradients was performed as follows. HEK293T cells were harvested with 100  $\mu\text{g}/\text{ml}$  cycloheximide/PBS. The cells were lysed in buffer B (20 mM HEPES-KOH (pH 7.5), 1 mM EGTA, 5 mM MgCl<sub>2</sub>, 150 mM KCl, 100  $\mu\text{g}/\text{ml}$  cycloheximide, protease inhibitor mixture (Nacalai Tesque), 0.5% Nonidet P-40, 0.5% Triton X-100, 0.5% sodium deoxycholate) on ice for 10 min. The cell extract was

centrifuged at 20,400  $\times g$  for 10 min, and the supernatant was layered over linear 10–50% sucrose density gradients in buffer C (20 mM HEPES-KOH (pH 7.5), 1 mM EGTA, 5 mM MgCl<sub>2</sub>, 150 mM KCl, and 100  $\mu\text{g}/\text{ml}$  cycloheximide) and centrifuged at 37,000 rpm for 90 min using a Beckman SW41Ti rotor. After centrifugation, 500- $\mu\text{l}$  fractions were collected using a BIO-COMP piston gradient fractionator.

#### Data availability

All data are contained within the article.

**Acknowledgments**—We thank the members of the Hoshino laboratory for technical assistance, reagents, and helpful discussions.

**Author contributions**—H. I. data curation; H. I. and N. H. formal analysis; H. I. and N. H. validation; H. I. and N. H. investigation; H. I. visualization; H. I., N. H., and S. H. writing-original draft; N. H. and H. T. methodology; N. H. writing-review and editing; H. T. resources; S. H. conceptualization; S. H. supervision; S. H. funding acquisition; S. H. project administration.

**Funding and additional information**—This work was supported by the Japan Society for the Promotion of Science (JSPS) Grant-in-Aid for Scientific Research (B) JP17H03635 (to S. H.), Program on the Innovative Development and the Application of New Drugs for Hepatitis B from the Japan Agency for Medical Research and development, AMED Grant JP17fk0310111 (to S. H.), and TAKEDA Science Foundation Grant JOSEI32912 (to S. H.).

**Conflict of interest**—The authors declare that they have no conflicts of interest with the contents of this article.

**Abbreviations**—The abbreviations used are: PAM2, PABPC1-interacting motif 2; ARE, adenine/uridine-rich element; CPE, cytoplasmic polyadenylation element; SCA2, spinocerebellar ataxia type 2; GST, glutathione S-transferase; BGG,  $\beta$ -globin; GAPDH, glyceraldehyde-3-phosphate dehydrogenase; EGFP, enhanced GFP; aa, amino acid(s); RL-PAT, RNA ligation-mediated poly(A) test; RT, reverse transcriptase; IP, immunoprecipitation; DIG, digoxigenin.

#### References

- Keller, W. (1995) No end yet to messenger RNA 3' processing! *Cell* **81**, 829–832 CrossRef Medline
- Goldstrohm, A. C., and Wickens, M. (2008) Multifunctional deadenylase complexes diversify mRNA control. *Nat. Rev. Mol. Cell Biol.* **9**, 337–344 CrossRef Medline
- Weill, L., Belloc, E., Bava, F. A., and Méndez, R. (2012) Translational control by changes in poly(A) tail length: recycling mRNAs. *Nat. Struct. Mol. Biol.* **19**, 577–585 CrossRef Medline
- Mangus, D. A., Evans, M. C., and Jacobson, A. (2003) Poly(A)-binding proteins: multifunctional scaffolds for the post-transcriptional control of gene expression. *Genome Biol.* **4**, 223 CrossRef Medline
- Imataka, H., Gradi, A., and Sonenberg, N. (1998) A newly identified N-terminal amino acid sequence of human eIF4G binds poly(A)-binding protein and functions in poly(A)-dependent translation. *EMBO J.* **17**, 7480–7489 CrossRef Medline
- Wells, S. E., Hillner, P. E., Vale, R. D., and Sachs, A. B. (1998) Circularization of mRNA by eukaryotic translation initiation factors. *Mol. Cell* **2**, 135–140 CrossRef Medline

**EDITORS' PICK: Ataxin-2 mediates cytoplasmic polyadenylation**

7. Uchida, N., Hoshino, S., Imataka, H., Sonenberg, N., and Katada, T. (2002) A novel role of the mammalian GSPT/eRF3 associating with poly(A)-binding protein in cap/poly(A)-dependent translation. *J. Biol. Chem.* **277**, 50286–50292 [CrossRef](#) [Medline](#)
8. Gallie, D. R. (1998) A tale of two termini: a functional interaction between the termini of an mRNA is a prerequisite for efficient translation initiation. *Gene* **216**, 1–11 [CrossRef](#) [Medline](#)
9. Gallie, D. R. (1991) The cap and poly(A) tail function synergistically to regulate mRNA translational efficiency. *Genes Dev.* **5**, 2108–2116 [CrossRef](#) [Medline](#)
10. Funakoshi, Y., Doi, Y., Hosoda, N., Uchida, N., Osawa, M., Shimada, I., Tsujimoto, M., Suzuki, T., Katada, T., and Hoshino, S. (2007) Mechanism of mRNA deadenylation: evidence for a molecular interplay between translation termination factor eRF3 and mRNA deadenylases. *Genes Dev.* **21**, 3135–3148 [CrossRef](#) [Medline](#)
11. Ikematsu, N., Yoshida, Y., Kawamura-Tsuzuku, J., Ohsugi, M., Onda, M., Hirai, M., Fujimoto, J., and Yamamoto, T. (1999) Tob2, a novel anti-proliferative Tob/BTG1 family member, associates with a component of the CCR4 transcriptional regulatory complex capable of binding cyclin-dependent kinases. *Oncogene* **18**, 7432–7441 [CrossRef](#) [Medline](#)
12. Okochi, K., Suzuki, T., Inoue, J., Matsuda, S., and Yamamoto, T. (2005) Interaction of anti-proliferative protein Tob with poly(A)-binding protein and inducible poly(A)-binding protein: implication of Tob in translational control. *Genes Cells* **10**, 151–163 [CrossRef](#) [Medline](#)
13. Uchida, N., Hoshino, S., and Katada, T. (2004) Identification of a human cytoplasmic poly(A) nuclease complex stimulated by poly(A)-binding protein. *J. Biol. Chem.* **279**, 1383–1391 [CrossRef](#) [Medline](#)
14. Yamashita, A., Chang, T. C., Yamashita, Y., Zhu, W., Zhong, Z., Chen, C. Y., and Shyu, A. B. (2005) Concerted action of poly(A) nucleases and decapping enzyme in mammalian mRNA turnover. *Nat. Struct. Mol. Biol.* **12**, 1054–1063 [CrossRef](#) [Medline](#)
15. Hoshino, S., Imai, M., Kobayashi, T., Uchida, N., and Katada, T. (1999) The eukaryotic polypeptide chain releasing factor (eRF3/GSPT) carrying the translation termination signal to the 3'-Poly(A) tail of mRNA: direct association of eRF3/GSPT with polyadenylate-binding protein. *J. Biol. Chem.* **274**, 16677–16680 [CrossRef](#) [Medline](#)
16. Osawa, M., Hosoda, N., Nakanishi, T., Uchida, N., Kimura, T., Imai, S., Machiyama, A., Katada, T., Hoshino, S., and Shimada, I. (2012) Biological role of the two overlapping poly(A)-binding protein interacting motifs 2 (PAM2) of eukaryotic releasing factor eRF3 in mRNA decay. *RNA* **18**, 1957–1967 [CrossRef](#) [Medline](#)
17. Decker, C. J., and Parker, R. (1993) A turnover pathway for both stable and unstable mRNAs in yeast: evidence for a requirement for deadenylation. *Genes Dev.* **7**, 1632–1643 [CrossRef](#) [Medline](#)
18. Lai, W. S., Carballo, E., Strum, J. R., Kennington, E. A., Phillips, R. S., and Blackshear, P. J. (1999) Evidence that tristetraprolin binds to AU-rich elements and promotes the deadenylation and destabilization of tumor necrosis factor  $\alpha$  mRNA. *Mol. Cell. Biol.* **19**, 4311–4323 [CrossRef](#) [Medline](#)
19. Sandler, H., Kreth, J., Timmers, H. T., and Stoecklin, G. (2011) Not1 mediates recruitment of the deadenylase Caf1 to mRNAs targeted for degradation by tristetraprolin. *Nucleic Acids Res.* **39**, 4373–4386 [CrossRef](#) [Medline](#)
20. Hosoda, N., Funakoshi, Y., Hirasawa, M., Yamagishi, R., Asano, Y., Miyagawa, R., Ogami, K., Tsujimoto, M., and Hoshino, S. (2011) Anti-proliferative protein Tob negatively regulates CPEB3 target by recruiting Caf1 deadenylase. *EMBO J.* **30**, 1311–1323 [CrossRef](#) [Medline](#)
21. Ogami, K., Hosoda, N., Funakoshi, Y., and Hoshino, S. (2014) Antiproliferative protein Tob directly regulates c-myc proto-oncogene expression through cytoplasmic polyadenylation element-binding protein CPEB. *Oncogene* **33**, 55–64 [CrossRef](#) [Medline](#)
22. Semotok, J. L., Cooperstock, R. L., Pinder, B. D., Vari, H. K., Lipshitz, H. D., and Smibert, C. A. (2005) Smaug recruits the CCR4/POP2/NOT deadenylase complex to trigger maternal transcript localization in the early *Drosophila* embryo. *Curr. Biol.* **15**, 284–294 [CrossRef](#) [Medline](#)
23. Goldstrohm, A. C., Hook, B. A., Seay, D. J., and Wickens, M. (2006) PUF proteins bind Pop2p to regulate messenger RNAs. *Nat. Struct. Mol. Biol.* **13**, 533–539 [CrossRef](#) [Medline](#)
24. Leppek, K., Schott, J., Reitter, S., Poetz, F., Hammond, M. C., and Stoecklin, G. (2013) Roquin promotes constitutive mRNA decay via a conserved class of stem-loop recognition motifs. *Cell* **153**, 869–881 [CrossRef](#) [Medline](#)
25. Geissler, R., Simkin, A., Floss, D., Patel, R., Fogarty, E. A., Scheller, J., and Grimson, A. (2016) A widespread sequence-specific mRNA decay pathway mediated by hnRNPs A1 and A2/B1. *Genes Dev.* **30**, 1070–1085 [CrossRef](#) [Medline](#)
26. Katoh, T., Hojo, H., and Suzuki, T. (2015) Destabilization of microRNAs in human cells by 3' deadenylation mediated by PARN and CUGBP1. *Nucleic Acids Res.* **43**, 7521–7534 [CrossRef](#) [Medline](#)
27. Rambout, X., Detiffe, C., Bruylants, E., Mariavelle, E., Cherkaoui, M., Brohee, S., Demoitié, P., Lebrun, M., Soini, R., Lesage, B., Guedri, K., Beullens, M., Bollen, M., Farazi, T. A., Kettmann, R., et al. (2016) The transcription factor ERG recruits CCR4-NOT to control mRNA decay and mitotic progression. *Nat. Struct. Mol. Biol.* **23**, 663–672 [CrossRef](#) [Medline](#)
28. Fukushima, M., Hosoda, N., Chifu, K., and Hoshino, S. I. (2019) TDP-43 accelerates deadenylation of target mRNAs by recruiting Caf1 deadenylase. *FEBS Lett.* **593**, 277–287 [CrossRef](#) [Medline](#)
29. Chen, C. Y., Zheng, D., Xia, Z., and Shyu, A. B. (2009) Ago-TNRC6 triggers microRNA-mediated decay by promoting two deadenylation steps. *Nat. Struct. Mol. Biol.* **16**, 1160–1166 [CrossRef](#) [Medline](#)
30. Fabian, M. R., Mathonnet, G., Sundermeier, T., Mathys, H., Zipprich, J. T., Svitkin, Y. V., Rivas, F., Jinke, M., Wohlschlegel, J., Doudna, J. A., Chen, C. Y., Shyu, A. B., Yates, J. R., 3rd, Hannon, G. J., Filipowicz, W., et al. (2009) Mammalian miRNA RISC recruits CAF1 and PABP to affect PABP-dependent deadenylation. *Mol. Cell* **35**, 868–880 [CrossRef](#) [Medline](#)
31. Zekri, L., Huntzinger, E., Heimstädt, S., and Izaurralde, E. (2009) The silencing domain of GW182 interacts with PABPC1 to promote translational repression and degradation of microRNA targets and is required for target release. *Mol. Cell. Biol.* **29**, 6220–6231 [CrossRef](#) [Medline](#)
32. Barnard, D. C., Ryan, K., Manley, J. L., and Richter, J. D. (2004) Symplekin and xGLD-2 are required for CPEB-mediated cytoplasmic polyadenylation. *Cell* **119**, 641–651 [CrossRef](#) [Medline](#)
33. Burns, D. M., D'Ambrogio, A., Nottrott, S., and Richter, J. D. (2011) CPEB and two poly(A) polymerases control miR-122 stability and p53 mRNA translation. *Nature* **473**, 105–108 [CrossRef](#) [Medline](#)
34. Novoa, I., Gallego, J., Ferreira, P. G., and Mendez, R. (2010) Mitotic cell-cycle progression is regulated by CPEB1 and CPEB4-dependent translational control. *Nat. Cell Biol.* **12**, 447–456 [CrossRef](#) [Medline](#)
35. Yamagishi, R., Tsusaka, T., Mitsunaga, H., Maehata, T., and Hoshino, S. (2016) The STAR protein QKI-7 recruits PAPD4 to regulate post-transcriptional polyadenylation of target mRNAs. *Nucleic Acids Res.* **44**, 2475–2490 [CrossRef](#) [Medline](#)
36. Fernandez, M., McClain, M. E., Martinez, R. A., Snow, K., Lipe, H., Ravits, J., Bird, T. D., and La Spada, A. R. (2000) Late-onset SCA2: 33 CAG repeats are sufficient to cause disease. *Neurology* **55**, 569–572 [CrossRef](#) [Medline](#)
37. Imbert, G., Saudou, F., Yvert, G., Devys, D., Trottier, Y., Garnier, J. M., Weber, C., Mandel, J. L., Cancel, G., Abbas, N., Dürr, A., Didierjean, O., Stevanin, G., Agid, Y., and Brice, A. (1996) Cloning of the gene for spinocerebellar ataxia 2 reveals a locus with high sensitivity to expanded CAG/glutamine repeats. *Nat. Genet.* **14**, 285–291 [CrossRef](#) [Medline](#)
38. Pulst, S. M., Nechiporuk, A., Nechiporuk, T., Gispert, S., Chen, X. N., Lopes-Cendes, I., Pearlman, S., Starkman, S., Orozco-Díaz, G., Lunkes, A., DeJong, P., Rouleau, G. A., Auburger, G., Korenberg, J. R., Figueiroa, C., et al. (1996) Moderate expansion of a normally biallelic trinucleotide repeat in spinocerebellar ataxia type 2. *Nat. Genet.* **14**, 269–276 [CrossRef](#) [Medline](#)
39. Sanpei, K., Takano, H., Igarashi, S., Sato, T., Oyake, M., Sasaki, H., Wakasaka, A., Tashiro, K., Ishida, Y., Ikeuchi, T., Koide, R., Saito, M., Sato, A., Tanaka, T., Hanyu, S., et al. (1996) Identification of the spinocerebellar ataxia type 2 gene using a direct identification of repeat expansion and cloning technique, DIRECT. *Nat. Genet.* **14**, 277–284 [CrossRef](#) [Medline](#)
40. Elden, A. C., Kim, H. J., Hart, M. P., Chen-Plotkin, A. S., Johnson, B. S., Fang, X., Armakola, M., Geser, F., Greene, R., Lu, M. M., Padmanabhan, A., Clay-Falcone, D., McCluskey, L., Elman, L., Juhr, D., et al. (2010) Ataxin-2 intermediate-length polyglutamine expansions are associated with increased risk for ALS. *Nature* **466**, 1069–1075 [CrossRef](#) [Medline](#)

41. Albrecht, M., and Lengauer, T. (2004) Survey on the PABC recognition motif PAM2. *Biochem. Biophys. Res. Commun.* **316**, 129–138 [CrossRef](#) [Medline](#)
42. Kozlov, G., Trempe, J. F., Khaleghpour, K., Kahvejian, A., Ekiel, I., and Gehring, K. (2001) Structure and function of the C-terminal PABC domain of human poly(A)-binding protein. *Proc. Natl. Acad. Sci. U. S. A.* **98**, 4409–4413 [CrossRef](#) [Medline](#)
43. Satterfield, T. F., and Pallanck, L. J. (2006) Ataxin-2 and its *Drosophila* homolog, ATX2, physically assemble with polyribosomes. *Hum. Mol. Genet.* **15**, 2523–2532 [CrossRef](#) [Medline](#)
44. Yokoshi, M., Li, Q., Yamamoto, M., Okada, H., Suzuki, Y., and Kawahara, Y. (2014) Direct binding of Ataxin-2 to distinct elements in 3' UTRs promotes mRNA stability and protein expression. *Mol. Cell* **55**, 186–198 [CrossRef](#) [Medline](#)
45. Kozlov, G., Safaei, N., Rosenauer, A., and Gehring, K. (2010) Structural basis of binding of P-body-associated proteins GW182 and ataxin-2 by the M $\ddot{\text{a}}$ lle domain of poly(A)-binding protein. *J. Biol. Chem.* **285**, 13599–13606 [CrossRef](#) [Medline](#)
46. Charlesworth, A., Meijer, H. A., and de Moor, C. H. (2013) Specificity factors in cytoplasmic polyadenylation. *Wiley Interdiscip. Rev. RNA* **4**, 437–461 [CrossRef](#) [Medline](#)
47. Schmidt, M. J., and Norbury, C. J. (2010) Polyadenylation and beyond: emerging roles for noncanonical poly(A) polymerases. *Wiley Interdiscip. Rev. RNA* **1**, 142–151 [CrossRef](#) [Medline](#)
48. Ciosk, R., DePalma, M., and Priess, J. R. (2004) ATX-2, the *C. elegans* ortholog of ataxin 2, functions in translational regulation in the germline. *Development* **131**, 4831–4841 [CrossRef](#) [Medline](#)
49. McCann, C., Holohan, E. E., Das, S., Dervan, A., Larkin, A., Lee, J. A., Rodrigues, V., Parker, R., and Ramaswami, M. (2011) The Ataxin-2 protein is required for microRNA function and synapse-specific long-term olfactory habituation. *Proc. Natl. Acad. Sci. U. S. A.* **108**, E655–E662 [CrossRef](#) [Medline](#)
50. Lim, C., and Allada, R. (2013) ATAXIN-2 activates PERIOD translation to sustain circadian rhythms in *Drosophila*. *Science* **340**, 875–879 [CrossRef](#) [Medline](#)
51. Zhang, Y., Ling, J., Yuan, C., Dubruille, R., and Emery, P. (2013) A role for *Drosophila* ATX2 in activation of PER translation and circadian behavior. *Science* **340**, 879–882 [CrossRef](#) [Medline](#)
52. Lastres-Becker, I., Nonis, D., Eich, F., Klinkenberg, M., Gorospe, M., Kötter, P., Klein, F. A., Kedersha, N., and Auburger, G. (2016) Mammalian ataxin-2 modulates translation control at the pre-initiation complex via PI3K/mTOR and is induced by starvation. *Biochim. Biophys. Acta* **1862**, 1558–1569 [CrossRef](#) [Medline](#)
53. Kwak, J. E., Drier, E., Barbee, S. A., Ramaswami, M., Yin, J. C., and Wickens, M. (2008) GLD2 poly(A) polymerase is required for long-term memory. *Proc. Natl. Acad. Sci. U. S. A.* **105**, 14644–14649 [CrossRef](#) [Medline](#)
54. Papin, C., Rouget, C., and Mandart, E. (2008) *Xenopus* Rbm9 is a novel interactor of XGld2 in the cytoplasmic polyadenylation complex. *FEBS J.* **275**, 490–503 [CrossRef](#) [Medline](#)
55. Ezzeddine, N., Chang, T. C., Zhu, W., Yamashita, A., Chen, C. Y., Zhong, Z., Yamashita, Y., Zheng, D., and Shyu, A. B. (2007) Human TOB, an anti-proliferative transcription factor, is a poly(A)-binding protein-dependent positive regulator of cytoplasmic mRNA deadenylation. *Mol. Cell. Biol.* **27**, 7791–7801 [CrossRef](#) [Medline](#)
56. Ruan, L., Osawa, M., Hosoda, N., Imai, S., Machiyama, A., Katada, T., Hoshino, S., and Shimada, I. (2010) Quantitative characterization of Tob interactions provides the thermodynamic basis for translation termination-coupled deadenylase regulation. *J. Biol. Chem.* **285**, 27624–27631 [CrossRef](#) [Medline](#)
57. Hosoda, N., Kim, Y. K., Lejeune, F., and Maquat, L. E. (2005) CBP80 promotes interaction of Upf1 with Upf2 during nonsense-mediated mRNA decay in mammalian cells. *Nat. Struct. Mol. Biol.* **12**, 893–901 [CrossRef](#) [Medline](#)